Turbulence-Flow Coupling and Poloidal Main-Ion Flow Acceleration Preceding the L-H Transition

L. Schmitz,[1] B. Grierson,[2] Z. Yan,[3] T.L. Rhodes,[1] G.R. McKee,[3] P. Gohil,[4] L. Zeng,[1] L. Bardoczi,[1] D. Eldon,[2] C. Chrystal,[4] K.H. Burrell,[4] C.C. Petty.[4]

[1]University of California Los Angeles, PO Box 957099, Los Angeles, CA 90095-7099, USA
[2]Princeton Plasma Physics Laboratory, PO Box 451, Princeton, NJ 08543-0451, USA
[3]University of Wisconsin-Madison, 1500 Engineering Dr., Madison, WI 53706, USA
[4]General Atomics, PO Box 85608, San Diego, CA 92186-5608, USA

email contact of main author: lschmitz@ucla.edu

A**bstract** It is shown here for the first time that the main-ion poloidal flow acceleration is quantitatively consistent with Reynolds-stress-driven shear flow amplification across the entire edge shear layer, leading to the observed dipolar shear layer structure inside the last closed flux surface (LCFS). It is demonstrated that the Reynolds stress gradient changes sign across the shear layer, consistent with the observed poloidal flow propagation in opposite directions. The measured Reynolds stress drive is quantitatively balanced by the ion flow acceleration and damping terms. The poloidal flow damping rate is found to be consistent with the neoclassical plateau regime for intermediate density $\langle n \rangle = 3 \times 10^{19}$ m^{-3}. Understanding flow drive and damping across the relevant ion collisionality range is crucial for connecting the L-H transition trigger physics to the macroscopic L-H power threshold scaling. This work in helium, hydrogen, and deuterium plasmas substantially extends previous work on L-H transitions induced via limit cycle oscillations (LCO), and on fast (regular) L-H transitions. We present direct, high resolution measurements of the poloidal and toroidal main ion flow during the trigger phase of the L-H transition, using helium main-ion CER. The measured $\boldsymbol{E}\times\boldsymbol{B}$ velocity modulation at the start of the LCO is in phase with the local ion poloidal velocity modulation, indicating flow in opposite directions just inside the LCFS and near the bottom of the E_r well. In contrast, the laboratory frame toroidal velocity is not significantly modulated during LCO. This data presents compelling quantitative evidence that the L-mode-LCO transition is triggered via $\boldsymbol{E}\times\boldsymbol{B}$ shear flow amplification mediated by the perpendicular Reynolds stress gradient. Long range toroidal flow correlations are observed to increase strongly concomitantly with the formation of a strong $\boldsymbol{E}\times\boldsymbol{B}$ flow at the L-mode-LCO or L-H transition. Compared to deuterium plasmas, flow correlation is weaker in hydrogen plasmas which also have a higher L-H transition power threshold.

1. Flow Acceleration via Turbulence-Flow Coupling

A strong jet flow just inside the last closed flux surface (LCFS) at the transition to high confinement mode is considered the crucial ingredient that allows the H-mode edge transport barrier to form. Previous work in a number of toroidal devices has indicated that this jet flow may be initially driven by turbulence self-organization in the L-mode boundary layer via the turbulent Reynolds stress gradient [1-6]. Understanding flow drive by turbulent structures present during the L-mode phase, as well as flow damping across the relevant ion collisionality range is crucial for understanding the H-mode trigger dynamics. Evidence for flow drive is often derived from the turbulence advection velocity dominated by the $\boldsymbol{E}\times\boldsymbol{B}$ flow perpendicular to the magnetic field, and the Reynolds stress gradient is typically evaluated from a two-point measurement with limited radial resolution. In the work presented here, the poloidal ion flow acceleration preceding the L-H transition is directly measured via main ion Charge Exchange Recombination Spectroscopy (CER) and is found to be quantitatively consistent with Reynolds-stress-driven shear flow amplification across the entire L-mode edge plasma layer (Figure 1), leading to the formation of the observed dipolar shear flow layer just inside the last closed flux surface (LCFS). The momentum source for

the poloidal flow acceleration is the radial gradient of the perpendicular turbulent Reynolds stress $\partial\langle\tilde{v}_r\tilde{v}_\theta\rangle/\partial r$ (described by equation (1), as discussed in more detail in [7]):

$$(1+2q^2)\frac{\partial\langle v_\theta\rangle}{\partial t} = -\frac{\partial\langle\tilde{v}_r\tilde{v}_\theta\rangle}{\partial r} - q^2\varepsilon^{-2}\gamma_D\left(\langle v_\theta\rangle - v_{\theta Neo}\right) \quad (1)$$

Poloidal flow damping is attributed to collisions and is quantitatively consistent with the damping rate in the neoclassical plateau regime. Here, q is the safety factor, and $\varepsilon = r/R$ is the inverse aspect ratio. γ_D is the poloidal flow damping rate in the appropriate collisionality regime, and $v_{\theta Neo} = K_1\partial T_i/\partial r(1/Z_i eB)$ is the neoclassical ion flow, with the collisionality-dependent constant K_1 [8].

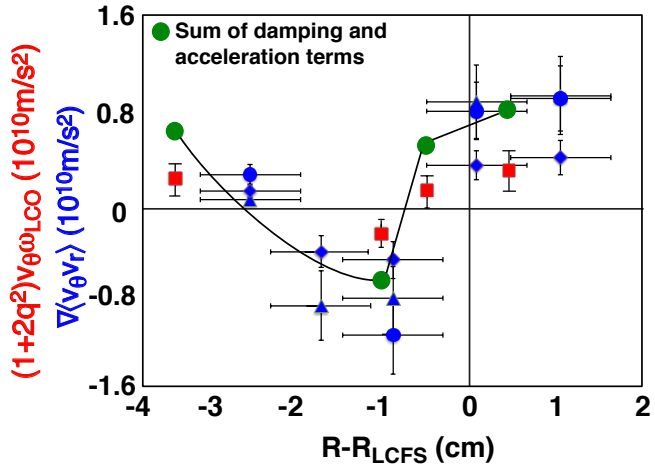

FIG. 1. Ion flow acceleration (from CER data, in red) and measured Reynolds stress gradients from BES (in blue), and the sum of the acceleration term and the calculated poloidal flow damping term according to equation (1) (in green), versus radius.

We present first a quantitative comparison of the measured poloidal ion flow acceleration, the driving Reynolds stress gradient and the neoclassical poloidal flow damping, allowing a detailed accounting of flow drive and damping across the edge electric field/shear layer. Fig. 1 shows the measured poloidal flow acceleration [in red- the left-hand of equation (1)] and the Reynolds stress gradient [in blue, the first right-hand term of eq. (1)], as well as the sum of the flow acceleration and damping (left-hand and second right-hand side) terms (in green), across the edge layer. The sum of flow acceleration and flow damping matches the Reynolds stress drive in sign and magnitude. The comparison reported here has been carried out in a helium plasma (single-null divertor with favorable ion grad-B drift towards the x-point, $B_\phi = 1.8T$, $\langle n\rangle = 3.5\times10^{19}$ m^{-3}, I_p= 0.8 MA, q_{95}=4.5), to enable main ion poloidal and toroidal flow measurements via CER. The plasma is heated by ~1.2 MW of ECH power and 1 MW of Neutral Beam co-injection (marginally above the L-H power threshold). Under these conditions, the L-mode phase transitions to an oscillatory state characterized by limit cycle oscillations (LCO) between the radial electric field and the tubulence level [shown in more detail in Figure 5(b-c)]. L-H transitions preceded by LCO allow investigating turbulence and flow interaction with high temporal and spatial resolution and have been previously studied in detail [1,2,4,9,10]. Here, experimental data enabling a detailed comparison of the terms in the momentum equation (1) were acquired across the edge electric field layer immediately after the L-mode-LCO transition. The poloidal flow acceleration is extracted from main-ion CER data, using the first four LCO cycles after the L-mode–LCO transition. An 8x8 chord Beam Emission Spectroscopy (BES) array with 1 cm radial/poloidal chord spacing is used to reconstruct the turbulent eddy flow pattern and derive the turbulent Reynolds stress.

Figure 2 shows that the ***E×B*** velocity modulation at the start of the LCO is in phase with the local ion poloidal velocity modulation just inside the LCFS (Fig.1; R~R_{LCFS}-0.7cm). Flow acceleration is positive (in the ion diamagnetic direction). Near the bottom of the E_r well (at R~R_{LCFS}-1.4cm), the poloidal main ion flow and the ***E×B*** flow are phase-shifted by ~150° indicating acceleration in the electron diamagnetic direction, consistent with the pattern in fig.1. A CER phase-lock analysis technique is used to extract the time-resolved poloidal and toroidal ion flow modulation in the early LCO phase. The ***E×B*** velocity is measured via Doppler Backscattering (DBS), and the density and ion temperature radial profiles via profile reflectometry and CER. Fig.2(a) shows that the measured poloidal ion flow modulation at the start of the LCO accounts within error margins for the measured ***E×B*** velocity modulation (the offset is due to L-mode diamagnetic flow and toroidal flow related to NBI co-injection). The modulation of the ion pressure gradient ∇P_i is negligible initially during the LCO phase [1,12] and during the initial (<100 μs) trigger phase of regular fast L-H transitions [5], but dominates ***E×B*** shear later in the transition sequence, locking in the H-mode transport barrier. The modulation of the laboratory frame toroidal main ion velocity [shown in Figure 2(b) as $v_\phi B_\theta / B_\phi$] is small, and out-of-phase compared to the poloidal velocity modulation. This result will be examined in more detail below.

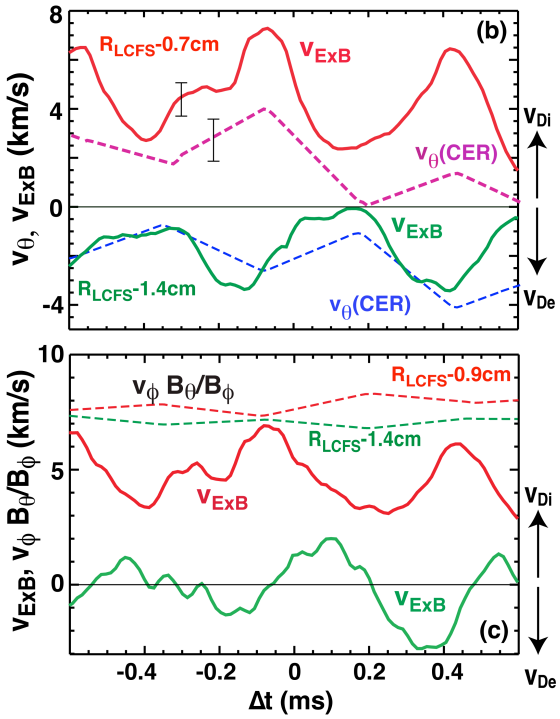

*FIG. 2. (a) Measured main ion poloidal velocity and **E×B** velocity in the outer shear layer (0.7 cm inside the LCFS) and near the center of the E_r well (1.4 cm inside the LCFS); (b) toroidal main ion velocity $v_\phi B_\theta / B_\phi$ and **E×B** velocity at the similar radii.*

Figure 3 shows the radial dependence of the flow damping rate across the edge layer, confirming that the plasma is in the plateau regime (characterized by $\gamma_T \varepsilon^{3/2} \le \nu_{ii} \le \gamma_T$ with the ion transit frequency $\gamma_T = v_{ith} / qR$ and the ion-ion collision rate ν_{ii}). The plateau regime flow damping rate is $\gamma_D = \gamma_T \varepsilon^{1/2}$. The sum of the measured flow acceleration and the plateau-regime damping rate calculated by using measured local plasma parameters is shown in Fig. 1 (green symbols). This data presents compelling quantitative evidence that the L-mode-LCO

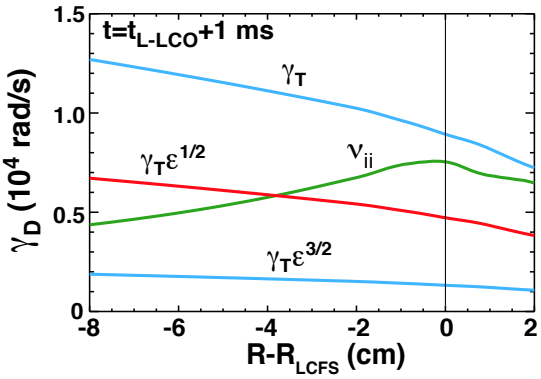

FIG. 3. The ion collisionality is in the plateau regime (ν_{ii} is below the ion transit frequency γ_T). The resulting neoclassical poloidal flow damping rate is indicated (red).

transition is triggered via $\boldsymbol{E}\times\boldsymbol{B}$ shear flow amplification mediated by the radial Reynolds stress gradient.

2. Toroidal Flow Decomposition

The lack of a large modulation of the measured laboratory frame toroidal ion velocity may be surprising at first if one considers that neoclassical toroidal flow damping is weak compared to poloidal flow damping. This observation can however be explained if the toroidal flow is decomposed into its respective components. The Pfirsch-Schlueter ion flow [11] parallel to the magnetic field ensures divergence-free flow in the flux-surface and constant pressure along the magnetic field lines. The parallel Pfirsch-Schlueter flow

$$v_{PS} = 2qv_{\perp}\cos\theta \qquad (2)$$

can be expressed in terms of the $\boldsymbol{E}\times\boldsymbol{B}$ and diamagnetic flow components given by

$$\vec{v}_{\perp} = \left(\vec{E}_r - \frac{\nabla p_i}{en_i}\right)\times\frac{\vec{B}}{B^2} \qquad (3)$$

Here, θ is the poloidal coordinate. The toroidal ion flow in the laboratory frame consists of the toroidal projection of the Pfirsch-Schlueter flow velocity

$$v_{\phi PS} = 2q\cos\theta\left(E_r - \frac{\nabla p_i}{en_i}\right)\frac{B_\phi}{B^2}$$

and the neutral-beam and intrinsically driven toroidal velocity, given by

$$v_{\phi d\_CER} = v_{\phi CER} - v_{\phi PS}$$

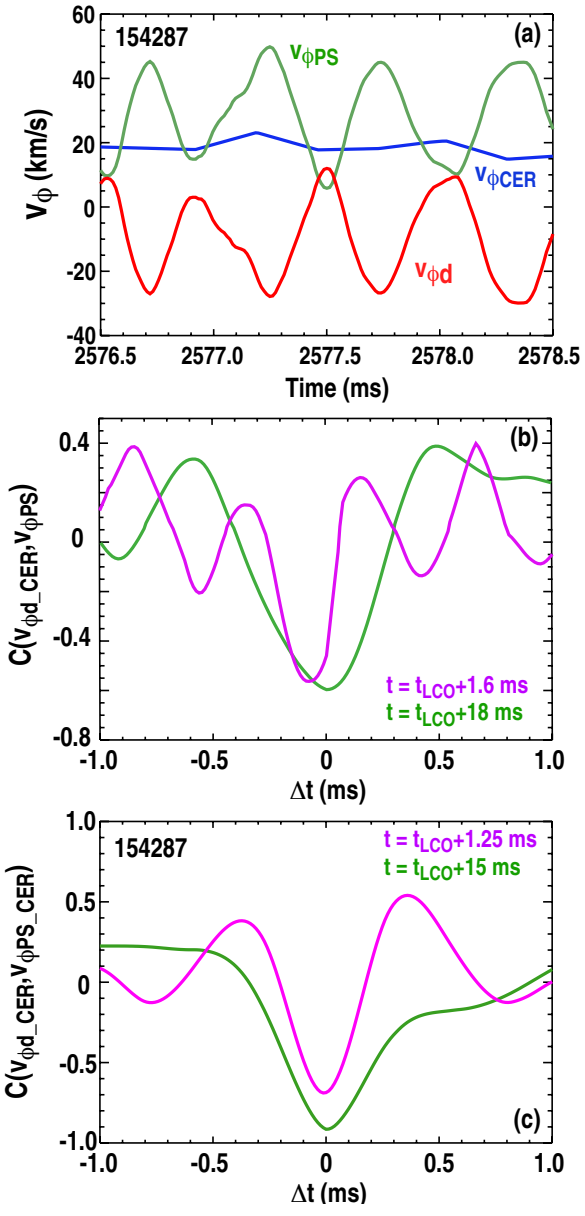

Fig.4: (a) Laboratory frame toroidal velocity (after subtraction of Pfirsch-Schlueter flow) and Pfirsch-Schlueter flow velocity. The total toroidal velocity measured in the laboratory frame via CER is also shown. (b) Cross correlation coefficient of toroidal flow velocity and Pfirsch-Schluter flow as measured by CER, for early and late LCO times, showing anti-correlation; (c) cross correlation coefficient between toroidal flow (CER) and Pfirsch-Schlueter flow as measured by DBS and profile reflectometry.

Here, $v_{\phi CER}$ is the measured (laboratory frame) toroidal velocity. The Pfirsch-Schluter flow can either be evaluated from equations (2,3) or directly from (lower time resolution) main ion CER poloidal flow data according to $v_{\phi PS\_CER} = 2q v_{\theta\_CER}(B_\phi / B)\cos(\theta)$.

Using equations (2,3), the ***E*×*B*** velocity is determined via the DBS Doppler shift measurement (here, as in the measurements shown in fig.2(a,b) we assume that the turbulence phase velocity is small compared to the ***E*×*B*** velocity; an assumption that has been shown to be valid except very close to the radius where E_r=0). All measurements are taken very close to the outboard midplane, so cos(θ) ~1. The radial plasma density gradient is evaluated with high (25 μs) time resolution from profile reflectometry, and the ion temperature and its radial gradient are determined via (carbon) CER data under the assumption that the Carbon ion temperature closely follows the main ion (He) temperature. Figure 4(a) shows that the toroidal velocity oscillates during the LCO when the Pfirsch-Schlueter toroidal flow contribution is subtracted from the laboratory frame toroidal rotation measured via main ion (He) CER (r/a~0.98). The Pfirsch-Schlueter flow, calculated from DBS and profile reflectometry data during the same time interval, exhibits a phase shift of ~ 180º. We have confirmed that this phase relationship holds at all times during the LCO. Fig. 4(b) shows that the toroidal velocity and the Pfirsch-Schlueter flow velocity are anti-correlated (this data is taken during a time interval ~2.5 ms immediately after the L-mode-LCO transition, and during a 2.5 ms interval ~18 ms after the L-mode-LCO transition (close to the LCO-H-mode transition). The Pfirsch-Schlueter flow is here evaluated from CER main ion poloidal rotation (as described above). Fig. 4(c) shows the correlation coefficient at similar times, but the Pfirsch-Schluter flow is in this case evaluated from the main ion poloidal velocity measured via CER. Figs. 4(b) and 4(c) differ somewhat due to the lower time resolution of the CER data (274 μs) but indicate clearly that approximate anti-correlation persists throughout the LCO phase.

3. Toroidal Flow Correlation

In the plasmas discussed so far, turbulence-driven flows and shear layer formation have been investigated in L-mode-LCO transitions in Helium plasmas, substantially extending previous work in DIII-D [1-2,6,9,12]. Now we consider long-range toroidal flow correlations. Previous experiments in several stellerators and tokamaks have shown that the toroidal correlation of flow fluctuations increases concomitantly with electrostatic biasing via an insertable or fixed electrode near the LCFS [13,14] and/or during spontaneous transport barrier formation (enhanced Ohmic confinement). Increasing long-range toroidal flow correlation is a characteristic signature for the development of large-scale, axisymmetric, turbulence-driven flows (Zonal Flows [15]) or turbulence-generated ion flows with poloidal/toroidal symmetry [1,9,12], and is hence expected when the L-H (or L-LCO) transitions are triggered.

Here we demonstrate that there are significant differences in the toroidal flow correlation in hydrogen and deuterium plasmas. Two different DBS channels with identical frequency but different toroidal launch positions (ϕ_1=60º and ϕ_2=240º) are used for this measurement. The characteristic increase of the long-range toroidal ***E*×*B*** flow correlation preceding the L-H

transition is found to be more pronounced in deuterium (D) plasmas as compared to hydrogen (H) at similar density. Figure 5(a) shows the time evolution of the cross correlation coefficient (at zero time delay) between the ***E***×***B*** velocity measured at r=0.95 at the two different toroidal positions in a deuterium plasma in ISS shape (ITER-similar shape).

No significant flow correlation is observed in L-mode prior to the L-mode-LCO transition. An expanded view of the ***E***×***B*** velocity and the correlation coefficient spanning this transition shows that the increase of the correlation coefficient occurs concomitantly with, or slightly precedes the development of oscillations in the ***E***×***B*** velocity at the transition to LCO. The maximum flow correlation coefficient is C~0.5-0.6. It is important to understand that the measured toroidal correlation implies toroidal as well as poloidal symmetry; following a fieldline, the rotational transform yields a difference in poloidal angle of ~ 60º between the two toroidally displaced outboard midplane DBS probing locations. There is no measurable toroidal correlation between the measured backscattered signal intensity (proportional to the density fluctuation power) as the poloidal correlation length is much smaller than the poloidal displacement between fieldlines intersecting both probing locations. The flow correlation appears to decrease at later times near the LCO- to H-mode transition. This is due to the fact that the DBS probing radius moves outwards radially as the density increases substantially once the H-mode pedestal begins to form. The radius probed after t=1808 ms is at the outer edge of the shear layer where toroidal correlation is lower.

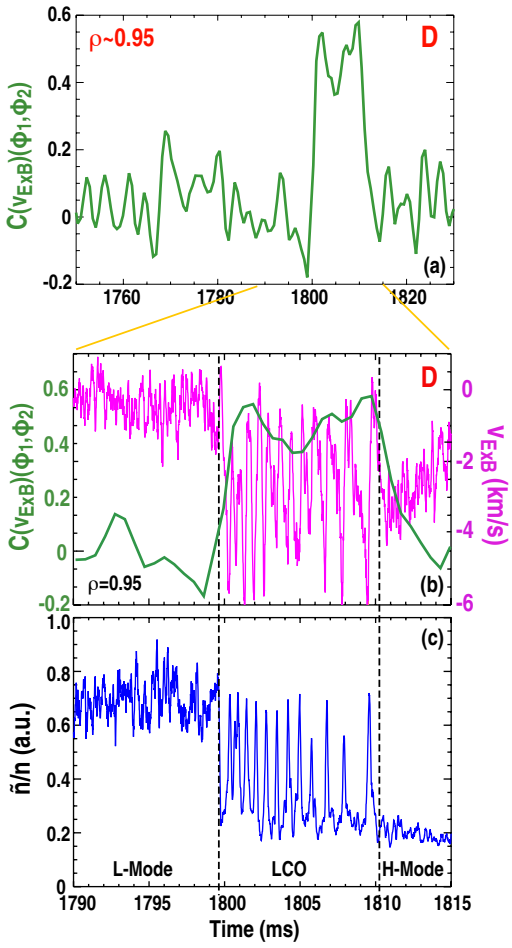

*FIG. 5. (a) Cross-correlation coefficient of the **E×B** velocities measured in a D plasma at the same minor radius at two different poloidal angles (ϕ=60º and ϕ=240º), with the same poloidal launch angle; (b) expanded time evolution of the correlation coefficient and the **E×B** velocity during the transition from L-mode to LCO; (c) time evolution of normalized density fluctuation level ñ/n across the L-mode-LCO-H-mode transitions.*

Similar data obtained in a hydrogen plasma is shown in Figure 6. This plasma has the same ITER-similar (ISS) shape and very similar density ($\langle n_e \rangle = 3\times10^{19}$ m^{-3}) than the deuterium plasma discussed previously. The toroidal flow correlation increases again concomitantly with the first transient in the edge ***E***×***B*** flow. In the case reported here, the plasma transitions directly to H-mode without intermediary LCO. However very similar results have been obtained in L-mode-LCO transitions in hydrogen plasmas. The maximum cross-correlation is C~0.3-0.4, and is consistently found to be substantially smaller compared

to deuterium plasmas, indicating that large-scale flows may not be generated as efficiently as in D-plasmas. The L-H transition power threshold in the ISS shape has been found to be 1.4-2 times higher in hydrogen plasmas compared to deuterium in the intermediate density range considered here. Less efficient flow drive in hydrogen would be consistent with an increased power threshold. Decreasing toroidal flow correlation has also been observed in TEXTOR Ohmic plasmas when the hydrogen- to deuterium fraction was increased [16]. In addition, long-range toroidal ***E***×***B*** flow correlation in DIII-D is observed to peak at intermediate plasma density around the L-H transition power threshold minimum and decreases at high and very low plasma density, further supporting a potential link between turbulence-flow coupling determining the L-H transition trigger and the power threshold density scaling.

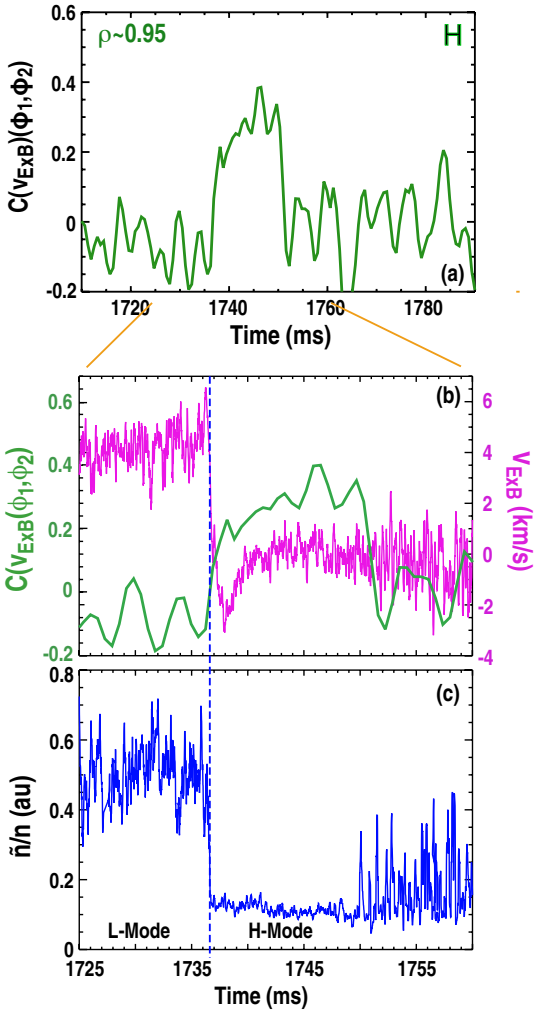

*FIG. 6. a) Toroidal cross-correlation of **E**×**B** flow in an H plasma (<n>=3x10^{13} cm^{-1}) across the L-H transition, showing a characteristic increase concomitantly with the negative excursion in the **E**×**B** drift (radial electric field) and the pronounced reduction in the density fluctuation level [Fig. 6(b,c)]. The changes well after the L-H transition are the result of the DBS probing radius moving outwards to larger minor radii.*

4. Conclusions

We have presented the first quantitative comparison of the measured poloidal ion flow acceleration, the driving Reynolds stress gradient and the neoclassical poloidal flow damping at the L-mode LCO transition, allowing a detailed accounting of flow drive and damping across the edge electric field layer. The dipolar nature of the edge flow layer has been clearly confirmed both via main ion CER measurements and via the Reynolds stress gradient determined from BES velocimetry analysis. It has been demonstrated that (i) the Reynolds stress gradient changes sign across the shear layer, consistent with the observed poloidal flow propagation in opposite directions; (ii) the measured Reynolds stress is quantitatively balanced by the flow acceleration and damping terms across the edge electric field layer. Poloidal main ion flow acceleration in the ion diamagnetic direction has been observed near the LCFS, and acceleration in the electron diamagnetic direction further inside the plasma near the bottom of the electric field well. It should be pointed out that after several initial LCO oscillation cycles, the ion pressure profile begins to steepen periodically at times when fluctuations are suppressed, as shown in detail in earlier work [1,9,12]. The diamagnetic ion flow hence

becomes increasingly more important as LCO evolve, and provides the crucial increase in edge $\boldsymbol{E}\times\boldsymbol{B}$ shear that facilitates the transition to sustained H-mode confinement.

The data presented here have been obtained at intermediate density near the L-H power threshold minimum. This work represents an important step towards developing a physics-based model of the L-H transition trigger and the L-H power threshold scaling. Further work is needed to extend these results to low and very high collisionality, in order to distinguish possible differences in L-mode turbulence properties and L-H transition trigger physics in the low density and high density branches of the power threshold scaling. The observed isotope dependence of the long-range toroidal flow correlation points towards substantial differences in L-mode turbulence properties preceding the transition. It appears that axisymmetric flows at the L-mode-LCO transition are less coherent and perhaps less well developed in hydrogen plasmas, compared to deuterium plasmas. Less efficient flow drive would make it more difficult to trigger the L-mode–LCO or the L-H transition, consistent with the substantially increased L-H transition power threshold in hydrogen. However other factors such as differences in the ion and electron radial thermal transport fluxes across the separatrix may also contribute to the increased power threshold in hydrogen. First principles gyrokinetic modeling of the L-mode state preceding the L-H transition will likely provide further insight into these differences.

This work is supported by the U.S. Department of Energy, under awards, DE-FG02-07ER54917[1], DE-AC02-09CH11466[2], DE-FG02-89ER53296[3] and DE-FC02-04ER54698[4]. DIII-D data shown in this paper can be obtained in digital format by following the links at https://fusion.gat.com/global/D3D_DMP.

[1] SCHMITZ, L., et al., Phys. Rev. Lett. **108**, 155002 (2012).
[2] TYNAN, G., et al., Nucl. Fusion **53**, 073053 (2013).
[3] MANZ, P., et al., 2012 Phys. Plasmas **19** 072311 (2012).
[4] XU, G.S., et al., Phys. Rev. Lett. **107** 125001 (2011).
[5] CZIEGLER, I., TYNAN, G.R., DIAMOND, P.H. et al., Plasma Phys. Control. Fusion **56** 075013 (2014).
[6] YAN, Z., et al., Phys Rev. Lett. **107**, 055004 (2014).
[7] DIAMOND, P.H. and KIM, Y.B., Phys. Fluids **B3**, 1626 (1991).
[8] KIM, Y.B., et al., Phys. Fluids **B3**, 2050 (1991).
[9] SCHMITZ, L., ZENG, L., RHODES, T.L., et al., Nucl. Fusion **54** 073012 (2014).
[10] MIKI, K., et al., Phys. Plasmas **19,** 092306 (2012).
[11] ASAKURA, N., SAKURAI, S., SHIMADA, M. et al., Phys. Rev. Lett. **84**, 3093 (2000).
[12] SCHMITZ, L., GRIERSON, B.A., ZENG, L., et al., paper EX/11-4, 25nd IAEA Fusion Energy Conference, Oct. 13-18, 2014, St. Petersburg, Russian Federation.
[13] PEDROSA, M.A., SILVA, C., HIDALGO, C., CARRERAS, B.A. et al., Phys. Rev. Lett. **100**, 215003 (2008).
[14] MANZ, P., RAMISCH, M. and STROTH, U., Physics of Plasmas **16**, 042309 (2009).
[15] DIAMOND, P.H., ITOH, S.I., ITOH, K. and HAHM, T.S., Plasma Phys. Control. Fusion **47**, R35 (2005).
[16] XU, Y., HIDALGO, C., SHESTERIKOV, I., et al., Phys. Rev. Lett. **110**, 265005 (2030).